Thermodynamic investigation of monoclonal antibody alkylated nucleoside interaction as a model for epitope recognition on nucleic acids

ARTICLE *in* BIOCHEMISTRY · MAY 1987

Impact Factor: 3.02 · DOI: 10.1021/bi00382a039 · Source: PubMed

6 AUTHORS, INCLUDING:

Stacieann C Yuhasz
U.S. Department of Veterans Affairs
19 PUBLICATIONS **200** CITATIONS
SEE PROFILE

Juergen Adamkiewicz
Philipps University of Marburg
31 PUBLICATIONS **882** CITATIONS
SEE PROFILE

Natl. Acad. Sci. U.S.A. 73, 2266-2269.
Jackson, V., Marshall, S., & Chalkley, R. (1981) *Nucleic Acids Res. 9*, 4563-4580.
Laemmli, U. K. (1970) *Nature (London) 227*, 680-683.
Laskey, R. A., & Mills, A. D. (1975) *Eur. J. Biochem. 56*, 335-342.
Leffak, I. M. (1983) *Nucleic Acids Res. 11*, 2717-2732.
Leffak, I. M. (1984) *Nature (London) 307*, 82-85.
Leffak, I. M., Grainger, R., & Weintraub, H. (1977) *Cell (Cambridge, Mass.) 12*, 837-846.
Russev, G., & Hancock, R. (1981) *Nucleic Acids Res. 9*, 4129-4137.
Seidman, M. M., Levine, A. J., & Weintraub, H. (1979) *Cell (Cambridge, Mass.) 18*, 439-449.
Senshu, T., Fukuda, M., & Ohashi, M. (1978) *J. Biochem. (Tokyo) 84*, 985-988.
Senshu, T., Yamasu, K., & Ohsawa, T. (1985) *Eur. J. Biochem. 150*, 575-580.
Simon, R. H., Camerini-Otero, R. D., & Felsenfeld, G. (1978) *Nucleic Acids Res. 5*, 4805-4818.
Sogo, J. M., Stahl, H., Koller, T., & Knippers, R. (1986) *J. Mol. Biol. 189*, 189-204.
Stein, A., Bina-Stein, M., & Simpson, R. T. (1977) *Proc. Natl. Acad. Sci. U.S.A. 74*, 2780-2784.
Stein, A., Whitlock, J. P., Jr., & Bina, M. (1979) *Proc. Natl. Acad. Sci. U.S.A. 76*, 5000-5004.
Worcel, A., Han, S., & Wong, M. L. (1978) *Cell (Cambridge, Mass.) 15*, 969-977.

Thermodynamic Investigation of Monoclonal Antibody Alkylated Nucleoside Interaction as a Model for Epitope Recognition on Nucleic Acids†

Stacieann C. Yuhasz,*,‡ Donald F. Senear,§ Jurgen Adamkiewicz,∥ Manfred F. Rajewsky,∥ Paul O. P. Ts'o,‡ and Lou-sing Kan‡

Division of Biophysics, The Johns Hopkins University, Baltimore, Maryland 21205, Department of Biology and McCollum-Pratt Institute, The Johns Hopkins University, Baltimore, Maryland 21218, and Institute of Cell Biology (Cancer Research), University of Essen, D-4300 Essen 1, West Germany

Received September 4, 1986; Revised Manuscript Received December 8, 1986

ABSTRACT: The objective of this investigation is examination of the dominant forces that govern complex formation between a series of monoclonal antibodies directed against O^6-ethyl-2′-deoxyguanosine. These monoclonal antibodies (coded as ER-6, ER-3, and EM-1) provide the basis for a thermodynamic comparative evaluation of the potentially different forces that stabilize the various monoclonal antibody (mAb) alkylated nucleoside complexes. The binding affinities of ER-6, ER-3, and EM-1 are measured in terms of specific (O^6-ethyl-2′-deoxyguanosine, or O^6-EtdGuo) and nonspecific (O^6-methyl-2′-deoxyguanosine, or O^6-MedGuo) antigens, under a variety of experimental conditions, including pH, sodium chloride addition, 1-propanol addition, and temperature, via a nitrocellulose affinity filter assay. The binding isotherms were analyzed via a least-squares routine fit to a two independent binding sites model. The temperature dependence of the van't Hoff enthalpies for the specific O^6-EtdGuo interaction ranges from −15.18 to −18.60 kcal mol^{-1}, while for O^6-MedGuo the range was extended from −2.72 to −20.66 kcal mol^{-1}. The standard and unitary entropies were negative for those mAb interactions with O^6-EtdGuo as well as for ER-6/O^6-MedGuo complex formation. However, it was found that the interactions between ER-3 and EM-1 with O^6-MedGuo led to decidedly positive entropic values. These results indicate two different dominant forces at work in complex stabilization. The interaction of the three mAb's with their specific antigen, as well as ER-6/O^6-MedGuo interaction (nonspecific), may well be controlled by van der Waals type forces, while ER-3 and EM-1 interactions with nonspecific antigen imply formal charge neutralization electrostatics as the dominant force.

The interactions between protein and DNA are recognized as important events in regulation of gene expression, DNA repair, and other biological processes. An understanding of the recognition mechanism that facilitates binding reactions between proteins and ligand(s) requires knowledge of the forces (hydrophobic, electrostatic, van der Waals, etc.) that govern the interactions. Hybridoma technology (Kohler & Milstein, 1976) has provided a means of obtaining specific monoclonal antibodies (mAb's) against alkylated nucleosides (Poirier, 1981; Baan et al., 1982; Adamkiewicz et al., 1982), thereby permitting thermodynamic and other biophysical studies on individual (nucleoside) epitope–mAb interactions. We have chosen a series of three monoclonal antibodies, each reactive against the alkylated nucleoside O^6-ethyl-2′-deoxyguanosine (Rajewsky et al., 1980; Muller & Rajewsky, 1981; Adamkiewicz et al., 1982), for a comparative thermodynamic evaluation of the forces that stabilize the mAb-alkylated nucleoside complex. Using this novel protein–DNA epitope interaction model, we are investigating whether structure–function relationships of this recognition phenomena can be

† This work was supported by NIH Grant 5T32 CA09110. Preliminary results of this work were presented at the 29th Annual Meeting of the Biophysical Society, Baltimore, MD, February 1985.
* Address correspondence to this author. This work is in partial fulfillment for the requirements of the Ph.D. degree from The School of Hygiene and Public Health, The Johns Hopkins University.
‡ Division of Biophysics, The Johns Hopkins University.
§ Department of Biology and McCollum-Pratt Institute, The Johns Hopkins University.
∥ University of Essen.

0006-2960/87/0426-2334$01.50/0

correlated to an underlying energetic pattern. It should be pointed out that no systematic thermodynamic investigation of mAb's with their antigens has been performed to date.

The binding affinities of two rat mAb's, ER-6 and ER-3, and one mouse mAb, EM-1, are measured in terms of specific (O^6-ethyl-2′-deoxyguanosine, or O^6-EtdGuo) and nonspecific (O^6-methyl-2′-deoxyguanosine, or O^6-MedGuo) antigens, under a variety of experimental conditions, including pH, temperature, sodium chloride concentration, and 1-propanol addition. The intrinsic binding constants (K_i) (Cantor & Schimmel, 1980) are evaluated by nitrocellulose affinity filter assay (NAFA) (Riggs et al., 1970), which has marked advantages over equilibrium dialysis (Garvey et al., 1977; Weir, 1978) as well as fluorescent techniques that require antigenic chromatofluors (Hobart & McConnell, 1975). The NAFA has the ability to yield quantitative free energy values of the protein–ligand interaction and facilitates rapid processing of the many samples requisite for a comprehensive thermodynamic characterization. The NAFA technique can be readily implemented at different desired temperatures, thus providing the means for enthalpy determination via the van't Hoff plot. NAFA binding isotherms obtained by this approach are analyzed by a nonlinear least-squares fitting procedure to obtain the K_i.

Materials and Methods

The mAb's (ER-6, ER-3, and EM-1) specific for O^6-EtdGuo were hybridoma culture supernatant derived and purified by affinity chromatography at the University of Essen as described previously (Rajewsky et al., 1980). The mAb's were examined for potential degradation after shipment to The Johns Hopkins University and at regular intervals during the course of these experiments, by 15% sodium dodecyl sulfate–polyacrylamide gel electrophoresis (SDS–PAGE) (Laemmli, 1970). Heavy and light chains (50 000 and 25 000 Da, respectively) were visualized in the gel by utilizing the Kodavue staining kit. The UPC120TA myeloma with unknown antigenicity was originally obtained from Litton Bionetics. The myeloma cells were proliferated in our laboratory by ascitic fluid production in syngeneic BALB/cπ mice (Potter, 1972). Purification of the myeloma antibody was achieved by a two-step 42% $(NH_4)_2SO_4$ precipitation, followed by extensive dialysis at 4 °C against 20 mM tris(hydroxymethyl)aminomethane (Tris), pH 7.2. The dialyzed protein was then separated into immunoglobulin and non-immunoglobulin fractions by DEAE-Affi-Gel blue chromatography at 4 °C utilizing a 0.0–400 mM NaCl gradient in 20 mM Tris, pH 7.2 (data not shown) (Bruck et al., 1982). The immunoglobulin components were fractionated into host (mouse) derived and UPC120TA myeloma antibody on a J. T. Baker poly(ethylenimine) (PEI) high-performance liquid chromatography (HPLC) anion-exchange column utilizing a 10–500 mM KH_2PO_4 gradient. Purity of the resulting fractions was confirmed by SDS–PAGE for one set of heavy and light chains. The UPC120TA was subtyped as $IgG_{2a,\lambda}$ (mouse immunoglobulin subtype identification kit, Boehringer Mannheim). The concentrations of ER-6, ER-3, EM-1, and UPC120TA antibodies were determined spectroscopically by using the extinction coefficient of IgG of 14.7 [1% w/v phosphate-buffered saline (PBS), 1 cm] (Ey, 1978).

The NAFA protocol routinely used consists of a type I titration of eleven serial dilutions of the appropriate mAb (150 μL) with a fixed amount of labeled specific or nonspecific antigen (150 μL) in 10 mM phosphate and 100 mM NaCl (unless otherwise specified) at the required temperature (7, 14, 25, 37 °C) for 2 h (equilibration) time in 1.5-mL microfuge tubes. The relative serial dilutions were based upon initial investigations of optimum mAb/antigen ratios to achieve saturation. To provide a measure of nonspecific binding effects, a 1:5000 dilution of UPC120TA was also incubated with the same labeled antigen (Mukker, 1984). In addition, a further control to check possible alterations in binding activity upon filter absorption was examined by variation in the washing times of the filter papers after application of the individual 100-μL samples, from 0.5 to 2.0 mL of buffer. This control led to no difference in the amount of counts bound per sample. Finally, the individual application times of the 100-μL samples are in no doubt slower than the first half-life of potential mAb–antigen dissociation, and if an alteration in the equilibrium status existed, the resulting counts bound would show significant deviations. During the incubation period, the nitrocellulose filters (Millipore HAWP 02500, 0.45 μM) were prepared by immersion in washing buffer [20 mM Tris-HCl, 2 mM ethylenediaminetetraacetic acid (EDTA), pH 7.5] also at the specified temperature. Those filters that did not readily wet were discarded, as previous studies indicate such filters exhibit lower protein–ligand retention capabilities. Following incubation, the solution complexes were microcentrifuged at 2000g for 2 min to assure all solution was available to be pipetted. It has been reported by Brenowitz et al. (1986) and confirmed independently by us that variation in pipetting aliquots of binding mixtures onto the filters is a major contribution to the standard deviation in the calculation of binding free energies. The prewetted filters were then applied to the Millipore filtration manifold (at the prescribed temperature), and solution complexes from three serial dilutions were loaded in triplicate (100 μL) on individual filters, affording analysis of nine filters simultaneously. House vacuum was administered until the filters appeared dry and then released while 1 mL of washing buffer (previously described) was added to each filter. The vacuum was readministered until the filters once again appeared dry. The 36 filters were subsequently placed in scintillation vials and dried at 80 °C for 1 h, or until filters appeared clear when 5 mL of scintillation cocktail (Betafluor, National Diagnostics) was added. The ^{3}H-labeled antigens used in each experiment were prepared by dilution of stock O^6-ethyl-2′-[^{3}H]deoxyguanosine (specific activity 34 Ci/mmol) (in part provided by Amersham) and O^6-methyl-2′-[^{3}H]-deoxyguanosine (specific activity 29 Ci/mmol) (Amersham) into the appropriate buffer at an activity such that mAb saturation was achieved (typically 2500 cpm/50 μL for O^6-EtdGuo vs. 10 000 cpm/50 μL for O^6-MedGuo with ER-6 mAb). Fifty microliters of the labeled antigen was applied to the prewetted filters and dried for the same duration. ^{3}H levels for the retained complexes were measured in a Beckman LS 7500 scintillation counter at 2% standard error.

The phosphate buffer stock solutions (pH 4–10) (Sigma Chemical Co.) were prepared by standard titration techniques and frequently filter sterilized (0.22 μM). 1-Propanol was obtained from Fisher, and NaCl was from Puratronic, Johnson Mathey Chemicals Ltd.

Data Analysis

The Binding Isotherm. The most general expression for the successive binding of ligands to two sites on a macromolecule is given by

$$\bar{Y}_t = \frac{K_1[L] + 2K_2[L]^2}{2(1 + K_1[L] + K_2[L]^2)} \quad (1)$$

where $\bar{Y}_t$ represents the fraction of total sites with bound ligand when the macromolecule (P) is in equilibrium with ligand at

activity [L]. K_1 and K_2 are macroscopic association constants as defined by eq 2 and 3 for the binding of one (K_1) or two (K_2) ligands.

$$K_1 = [P{\cdot}L]/[P][L] \quad (2)$$

$$K_2 = [PL_2]/[P][L]^2 \quad (3)$$

Assumptions. In analyzing our data, we have made the following simplyfying assumptions: (1) The law of mass action is obeyed. (2) The protein molecule does not affect the activity of the ligand except by binding. (3) The chemical activity of binding sites is unaffected by potential interactions between antibody molecules. (4) The activities and molar concentrations of antibody can be used interchangeably under the implication that ligand solutions of biochemical interest are ideally dilute. (5) The two binding sites on the antibody are equal and function independently of each other (Mukker, 1984).

The last assumption allows the macroscopic binding parameters to be replaced by a microscopic equilibrium constant describing the intrinsic affinity of an antigen for an antibody binding site.

$$K_1 \equiv 2K_i \quad (4)$$

$$K_2 \equiv K_i^2 \quad (5)$$

Rearrangement and substitution of the general binding expression (1) with eq 4 and 5 result in

$$\bar{Y}_t \equiv \frac{2K_i[L] + 2K_i^2[L]^2}{2(1 + 2K_i[L] + K_i^2[L]^2)} \quad (6)$$

Nitrocellulose filters retain protein molecules (antibody), hence those antigens bound to antibody binding sites, but not free antigen. Thus, when an equilibrium mixture of antibody and radioactively labeled antigen is drawn through such a filter, the radioactivity of the filter is proportional to the molar concentration of bound antigen. This quantity is given by the numerator of eq 6. Thus, the observed radioactivity of the filter is given by θ, where

$$\theta \equiv \gamma[P](2K_i)[L](1 + K_i) + \psi \quad (7)$$

The proportionality constant γ reflects both the efficiency with which the nitrocellulose filters retain antibody molecules (Woodbury & von Hippel, 1983) and the specific radioactivity of the labeled antigen. The former was routinely about 95% in our experiments. ψ represents the nonspecific antigen background filter binding retained by the filters in the absence of the antibody molecules in the equilibrium mixture. This antigen (Ag) background was routinely less than 1% of the total applied radioactivity. θ refers to the specific mAb–Ag complex retention corrected for the nonspecific antibody binding as suggested by Mukkur (1984). Thus, θ was expressed as the $cpm_{measured} - cpm_{UPC120TA}$, where $cpm_{measured}$ refers to ER-6, ER-3, and EM-1 interaction with O^6-EtdGuo or O^6-MedGuo and $cpm_{UPC120TA}$ is that binding by UPC120TA with no specificity for either of the aforementioned antigens.

The binding data were analyzed according to eq 7 by using nonlinear least-squares methods of parameter estimation (Johnson et al., 1976; Turner et al., 1981) to estimate the intrinsic binding constant, K_i, and its 65% confidence interval. For the type I titration used, it should be noted that $[L]_T \neq [L]$ and $[P]_T \neq [P]$. To solve for [L] and [P] for eq 7 as a function of $[P]_T$ and $[L]_T$, the two conservation equations given by

$$[P]_T \equiv [P] + [PL] + [PL_2] \quad (8)$$

$$[L]_T \equiv [L] + [PL] + 2[PL_2] \quad (9)$$

and the definitions of the macroscopic binding parameters K_1 and K_2 in eq 2–5 were rearranged as a cubic in [L]:

$$K_i^2[L]^3 + (2K_i[L]^2 + 2K_i^2[P]_T[L]^2 - [L]_TK_i^2[L]^2) + ([L] + [P]_T(2K_i)[L] - [L]_T(2K_i)[L]) - [L]_T = 0 \quad (10)$$

At each iteration of the nonlinear least-squares procedure, the current estimate of K_i was used to solve eq 10 for [L], utilizing Newton's method (Sorenson, 1980). [P] was then calculated from eq 8. These values of [L] and [P] were then incorporated into eq 7 for the next iteration of the least-squares procedure. The variance of the final fitted curve and the distribution of residuals were utilized to assess the goodness of fit. All calculations were performed on a Hewlett-Packard 1000 system, for each set (36 observations) of serially diluted mAb with the respective antigen, and repeated 3 times, resulting in three independent determinations of K_i. The binding isotherms (Figure 1) and remaining figures (Figures 2–4) are the average of nine determinations resulting from three independent experiments.

Binding free energies were calculated by the classic equation:

$$\Delta G^{\circ 1} = -RT \ln K_i \quad (11)$$

where $\Delta G^{\circ 1}$ is the apparent Gibbs free energy determined from the intrinsic affinity constant (Adair, 1925). We have chosen to use $\Delta G^{\circ 1}$ to describe these mAb–antigen systems, since protein–ligand equilibria often depend on many factors such as pH, salts, buffering compounds, etc., and since the net influence on K_i is seldom known. It is also worth mentioning that mAb's are a breed apart, due to the slightly different binding sites associated with their hypervariable domains. Apparent standard enthalpies were obtained from a linear analysis of the temperature dependence of the K_i, by means of the van't Hoff equation:

$$\partial \ln K_i/\partial(1/T) = -(\Delta H^{\circ 1}/R) \quad (12)$$

Results

Monoclonal antibodies designated as ER-6, ER-3, and EM-1 were obtained from the immunization of BDIX rats or Balb/c mice with O^6-EtdGuo coupled via the sodium periodate/sodium borohydride procedure (Erlanger & Beiser, 1964) to keyhole limpet hemocyanin (Muller & Rajewsky, 1980). After cloning of the hybridoma, the mAb's purified by affinity chromatography were subjected to an intensive and thorough radioimmunoassay competition screen to ascertain their specificity and cross-reactivity to a variety of closely related structures compared to the parent, O^6-EtdGuo (data not shown). It was from this original investigation that O^6-MedGuo was chosen as the nonspecific antigen due to its structural similarity to O^6-EtdGuo, sufficient cross-reactivity, and potential application for in vivo diagnostic procedures for the detection of alkylation–DNA adducts.

The original binding data analysis for this paper was like that proposed by Van Heyninger et al. (1983) for a type I titration described by eq 2. At the half-saturation point of the titration binding curve, the bound protein was defined as half of the total ligand concentration, where

$$[P{\cdot}L] \equiv [L]_T/2 \quad (13)$$

and the equilibrium constant was therefore obtained as

$$K_1 \equiv 1/[P] \quad (14)$$

This type of analysis, while useful as a first approximation of the binding constant, is not satisfactory to obtain accurate intrinsic binding affinities or, hence, free energies. Exami-

Table I: Effect of pH on Macroscopic Binding Affinities and Free Energies for ER-6, ER-3, and EM-1 Monoclonal Antibodies[a]

antigen		pH 4	pH 6	pH 7	pH 8	pH 10
			ER-6			
O^6-EtdGuo[e]	$K_1 \times 10^{-8}$ [b]	2.12	2.32	3.22	2.90	2.88
	$K_2 \times 10^{-16}$ [c]	1.12	1.35	2.59	2.10	2.07
	$\Delta G^{\circ 1}$ [d]	−10.94 ± 0.80	−11.00 ± 0.37	−11.21 ± 0.46	−11.13 ± 0.50	−11.12 ± 0.75
O^6-MedGuo[f]	$K_1 \times 10^{-7}$ [b]	1.67	1.06	1.36	1.23	0.89
	$K_2 \times 10^{-14}$ [c]	0.70	0.28	0.46	0.38	0.20
	$\Delta G^{\circ 1}$ [d]	−9.44 ± 0.18	−9.17 ± 0.16	−9.23 ± 0.16	−9.26 ± 0.11	−9.07 ± 0.07
			ER-3			
O^6-EtdGuo[e]	$K_1 \times 10^{-8}$ [b]	3.74	2.50	2.82	1.92	2.62
	$K_2 \times 10^{-16}$ [c]	3.50	1.56	1.99	0.92	1.74
	$\Delta G^{\circ 1}$ [d]	−11.28 ± 0.09	−11.04 ± 0.08	−11.11 ± 0.07	−10.88 ± 0.11	−11.07 ± 0.08
O^6-MedGuo[f]	$K_1 \times 10^{-8}$ [b]	1.38	1.92	0.80	5.92	2.38
	$K_2 \times 10^{-16}$ [c]	0.48	0.92	0.16	8.76	1.42
	$\Delta G^{\circ 1}$ [d]	−10.69 ± 0.11	−10.88 ± 0.15	−10.36 ± 0.08	−11.55 ± 0.14	−11.01 ± 0.14
			EM-1			
O^6-EtdGuo[e]	$K_1 \times 10^{-7}$ [b]	4.04	3.04	3.30	3.60	4.09
	$K_2 \times 10^{-14}$ [c]	4.08	2.31	2.72	3.24	4.18
	$\Delta G^{\circ 1}$ [d]	−9.96 ± 0.14	−9.79 ± 0.14	−9.84 ± 0.15	−9.89 ± 0.13	−9.96 ± 0.11
O^6-MedGuo[f]	$K_1 \times 10^{-6}$ [b]	4.58	7.50	10.30	20.40	7.80
	$K_2 \times 10^{-12}$ [c]	5.42	14.10	26.70	104.00	15.20
	$\Delta G^{\circ 1}$ [d]	−8.67 ± 0.21	−8.96 ± 0.13	−9.15 ± 0.03	−9.56 ± 0.13	−8.99 ± 0.16

[a] Conditions for all values in the table are as follows: 10 mM phosphate, 100 mM NaCl, 25 °C. [b] Macroscopic equilibrium contant (M^{-1}) for one bound antigen, $K_1 \equiv 2K_i$. [c] Macroscopic equilibrium constant (M^{-1}) for two bound antigens, $K_2 \equiv K_1^2$. [d] Apparent Gibbs free energy (kcal mol^{-1}) evaluated from $\Delta G^{\circ 1} \equiv -RT \ln K_i$. [e] O^6-Ethyl-2′-deoxyguanodine, the specific antigen. [f] O^6-Methyl-2′-deoxyguanosine, the nonspecific antigen.

nation of this type of analysis for a two-site system shows no simple relationship between either total antibody concentration $[P]_T$ or total ligand concentration $[L]_T$ at the half-saturation point with respect to any macroscopic equilibrium constant (K_1 or K_2). Therefore, we have utilized eq 1, the classical binding isotherm, for a more accurate model of mAb–ligand interaction and for the calculation of the intrinsic affinity constants.

pH Dependence. Table I demonstrates the effect of pH on the macroscopic affinity constants (K_1, K_2) and apparent Gibb's free energy ($\Delta G^{\circ 1}$) under standard buffer conditions (10 mM phosphate, 100 mM NaCl) at 25 °C. The $\Delta G^{\circ 1}$ calculated from the intrinsic equilibrium constants (K_i) are given in kcal mol^{-1} and reflect an average of nine experimental determinations which are accurate within the specified error limits. In confirmation of the competition studies, binding of O^6-EtdGuo is greater than that of O^6-MedGuo for all three mAb's, although the averaged relative binding ratio of O^6-EtdGuo/O^6-MedGuo is different for each mAb. The averaged binding ratios (pH 4–10, Table I) are 21.69, 1.10, and 3.57 for ER-6, ER-3, and EM-1, respectively. The macroscopic constants (K_1) are averaged within pH 4–10 since variation within this pH range is minimal. Thus, ER-6 exhibits the largest differential affinity in binding of O^6-EtdGuo to O^6-MedGuo, while ER-3 and EM-1 bind both antigens with nearly the same affinity. These differences in affinity are more accurately reflected in the free energies of association of the mAb–antigen complexes at pH 7, where $\Delta G^{\circ 1}$ ranges from −11.21 to −9.84 kcal mol^{-1} for O^6-EtdGuo and from −10.36 to −9.15 kcal mol^{-1} for O^6-MedGuo. Figure 1 shows two plots of the classical binding isotherms given by eq 1 of all three mAb's with both antigens for data at pH 7 and 25 °C. The isotherms, curve fit by nonlinear least-squares analysis, cover a three log range of mAb concentration and accurately reflect the trends of $\Delta G^{\circ 1}$ seen in Table I. θ, as mentioned previously, reflects the total radioactivity bound less nonspecific radioactivity, measured with the appropriate labeled antigen and nonspecific antibody, UPC120TA. Figure 1a, of O^6-EtdGuo binding isotherms, mirrors the $\Delta G^{\circ 1}$ of −11.21, −11.11, and −9.84 kcal mol^{-1} for ER-6, ER-3, and EM-1 interaction, respectively, while Figure 1b, for O^6-MedGuo binding, shows the $\Delta G^{\circ 1}$ of −10.36, −9.37, and −9.15 kcal mol^{-1} for ER-3, ER-6, and EM-1, indicative of a slight reduction in affinity. Variations in the binding isotherms for all other pH values (data not shown) reflect the favorable $\Delta G^{\circ 1}$ energies of Table I but in general demonstrate no enhanced free energy preference.

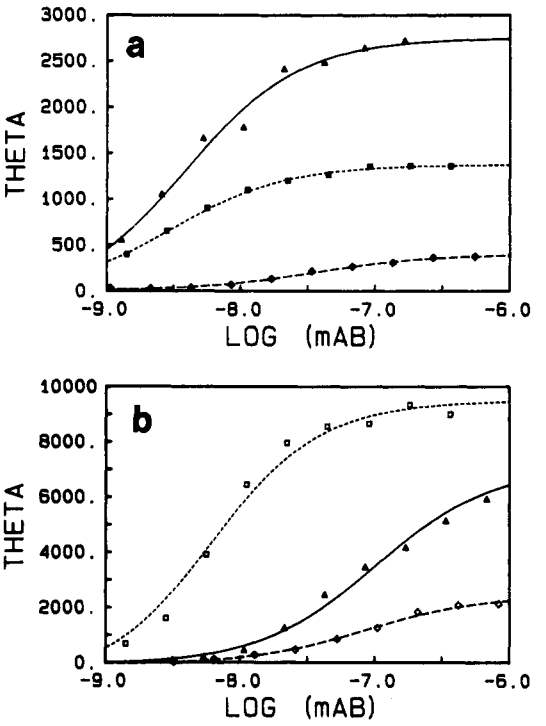

FIGURE 1: Binding isotherms for O^6-EtdGuo (a) and O^6-MedGuo (b) interaction with monoclonal antibodies ER-6 (triangles), ER-3 (squares), and EM-1 (diamonds) at pH 7, 10 mM phosphate, 100 mM NaCl, and 25 °C. Data points represent the average of nine trials and isotherms fit by nonlinear least-squares analysis to eq 7 (see Materials and Methods). Table I lists K_1 values.

Table II: Effect of Sodium Chloride on Macroscopic Binding Affinities and Free Energies[a]

antigen		[NaCl] (mM) 2.5 × 10¹	1 × 10²	5 × 10²	1 × 10³	1.5 × 10³
		ER-6				
O^6-EtdGuo	$K_1 \times 10^{-8}$	2.28	3.22	5.56	7.02	7.30
	$K_2 \times 10^{-16}$	1.30	2.59	7.73	12.30	13.30
	$\Delta G°_1$	−11.12 ± 0.14	−11.21 ± 0.46	−11.51 ± 0.13	−11.65 ± 0.18	−11.67 ± 0.15
O^6-MedGuo	$K_1 \times 10^{-7}$		1.36		3.54	
	$K_2 \times 10^{-14}$		0.46		3.13	
	$\Delta G°_1$		−9.32 ± 0.12		−9.88 ± 0.18	

antigen		[NaCl] (mM) 2.5 × 10¹	5.0 × 10¹	1 × 10²	1.5 × 10³
		ER-3			
O^6-EtdGuo	$K_1 \times 10^{-8}$	2.80	2.76	2.82	3.34
	$K_2 \times 10^{-16}$	1.96	1.90	1.99	2.79
	$\Delta G°_1$	−11.11 ± 0.14	−11.10 ± 0.09	−11.11 ± 0.7	−11.21 ± 0.17
O^6-MedGuo	$K_1 \times 10^{-7}$	1.32	1.01	7.96	
	$K_2 \times 10^{-14}$	0.44	0.65	15.80	
	$\Delta G°_1$	−9.30 ± 0.12	−9.41 ± 0.09	−10.36 ± 0.8	

antigen		[NaCl] (mM) 2.5 × 10¹	5.0 × 10¹	1 × 10²	1.5 × 10³
		EM-1			
O^6-EtdGuo	$K_1 \times 10^{-7}$	2.20	2.22	3.30	2.70
	$K_2 \times 10^{-14}$	1.21	1.23	2.72	1.82
	$\Delta G°_1$	−9.60 ± 0.15	−9.61 ± 0.14	−9.84 ± 0.12	−9.72 ± 0.15
O^6-MedGuo	$K_1 \times 10^{-6}$	2.10	3.26	10.30	
	$K_2 \times 10^{-12}$	1.10	2.66	26.70	
	$\Delta G°_1$	−8.21 ± 0.18	−8.47 ± 0.21	−9.15 ± 0.03	

[a] Conditions for all values in the table are as follows: pH 7.0, 10 mM phosphate, 25 °C.

Sodium Chloride Effect. Table II and Figure 2 present the effect of a monovalent salt on the binding equilibria, from low to moderate sodium chloride concentrations in 10 mM phosphate buffer, pH 7.0 and 25 °C. It was found by dialysis experiments that exposure to salt 2 M and higher resulted in irreversible denaturation of the mAb's as judged by NAFA binding, thereby limiting the range of salt concentrations that can be investigated.

The general equation for the effect of a low-molecular-weight substance (salt) on a macromolecular equilibria is given by

$$(\mathrm{d} \ln K_i)/(\mathrm{d} \ln [\mathrm{X}]) \equiv \Delta\bar{x} - (n_x/n_w)\Delta\bar{w} \qquad (15)$$

where [X] is the molar salt concentration, n_x and n_w represent the mole fractions of salt and water, respectively, and $\Delta\bar{x}$ and $\Delta\bar{w}$ represent the changes in the number of bound salt and water molecules that accompany the binding reaction (Tanford, 1969). If the effect of hydration is not considered, the above equation simplifies on the right side to $\Delta\bar{x}$, which has been utilized by several investigators to explain the loss of protons upon binding and formation of specific electrostatic contacts between the mAb and its antigen (Daune, 1972; Casperson & Voss, 1983; Porschke & Rauh, 1983; Johnston et al., 1985).

Figure 2 demonstrates the effect of increasing sodium chloride concentration on binding of both O^6-EtdGuo and O^6-MedGuo to the three mAb's. Figure 2a shows positive shallow slopes (2.47×10^{-1}, 4.67×10^{-2}, and 4.95×10^{-2} for ER-6, ER-3, and EM-1, respectively) fit by linear least-squares analysis for binding of O^6-EtdGuo, while Figure 2b presents a similar shallow slope for ER-6 (4.17×10^{-1}) and significantly steeper slopes for ER-3 and EM-1 interaction with O^6-MedGuo (1.29 and 1.79, respectively). Interpretation of these results implies marginal electrostatic contributions for O^6-EtdGuo interaction with all mAb's as well as O^6-MedGuo interaction with ER-6. However, ER-3 and EM-1 binding to O^6-MedGuo demonstrates enhanced affinities at higher sodium

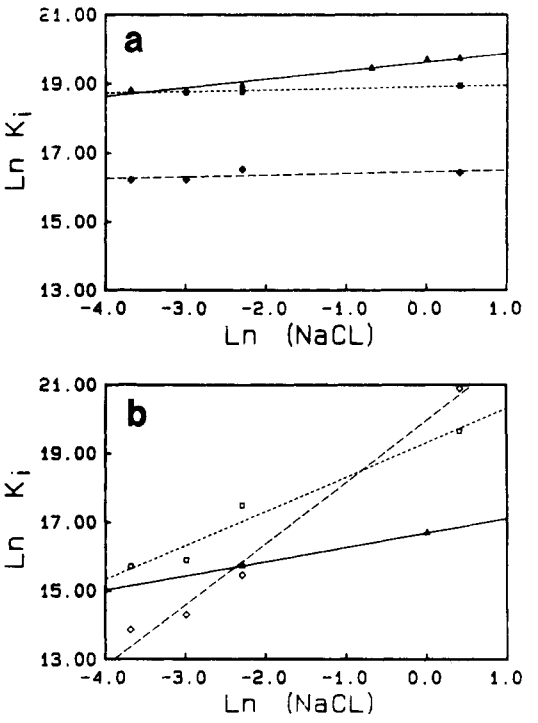

FIGURE 2: Effect of sodium chloride on ln K_i for O^6-EtdGuo (a) and O^6-MedGuo (b) with ER-6, ER-3, and EM-1 monoclonal antibodies, at pH 7, 10 mM phosphate, and 25 °C. Symbols denote same connotations as in Figure 1. Slopes were curve fit by linear least-squares analysis, and Table II lists values.

chloride concentration, indicative of an electrostatic component in the summation of forces that control complex formation. The O^6-EtdGuo and O^6-MedGuo/ER-6 (shallow positive slopes) are indicators that formal charge association is not the dominant force necessary for recognition and subsequent stable interaction. However, since the slopes do exhibit slight enhancement at higher salt concentrations, it is not possible to

eliminate other electrostatic forces such as dipole–dipole or ion–dipole components from the summation of contributions of all forces. Such forces would experience an attenuated effect in the presence of increased salt compared to formal charges, due to the lack of defined charge centers. It is also possible that the salt effect is exerted directly on protein conformation, which indirectly affects the interaction between the mAb binding sites and the antigen. The steeper salt slopes of O^6-MedGuo with mAb's ER-3 and EM-1 are interesting, implying alternate dominant forces at work compared to O^6-EtdGuo interaction. The steep slopes exhibited in Figure 2b are characteristic of formal charge interaction that is stabilized by compensating charge clusters at higher salt concentrations. While the antigen O^6-MedGuo has no formal charge at neutral pH, it is quite probable that formal charges within the antigen combining site or at other regions are responsible for this effect.

Propanol Effect. In 1937, H. C. Hamaker presented a theory to interpret colloid stability whereby the London–van der Waals force could be split into a purely geometrical part and a constant A, called the Hamaker constant, which depends only on the materials involved:

$$\Delta F(d_0) \equiv -A/(12\pi d_0) \qquad (16)$$

where ΔF corresponds to the interfacial interaction energy at separation distance d_0, for macromolecules represented as an interaction between two semi-infinite slabs. From eq 16, it is evident that if the system (macromolecules plus solvent) Hamaker coefficient is negative, the interactions between any two or more substances will be positive and the interfacial interaction energy no longer favored. By use of the individual Hamaker coefficients for two macromolecules (M_1 and M_2, with Hamaker coefficients A_{11} and A_{22}, respectively) dissolved in water (A_{33}), ΔF will be repulsive when either of the following conditions exist (Hamaker, 1937; van Oss et al., 1979):

$$A_{11} > A_{33} > A_{22}$$

or

$$A_{11} < A_{33} < A_{22}$$

Therefore, when two macromolecules are dissolved in water, M_1 and M_2 will experience a van der Waals repulsion ($+\Delta F$) when the interactions between each macromolecule and water are larger than the interactions between the macromolecules themselves. However, biological macromolecules in general have a lower interfacial interaction energy than water (van Oss et al., 1979), resulting in violation of the repulsion conditions and consequent van der Waals attractions. 1-Propanol addition lowers the surface tension (dynes per centimeter) of the water (Weast, 1981), which is directly proportional to the interfacial interaction energy, thereby reestablishing A_{33} as intermediary between the two macromolecules' Hamaker coefficients. The aftermath of varying concentrations of 1-propanol addition is van der Waals attractions turned repulsive and a minimal partial specific volume charge associated with alcohol addition to aqueous solutions (Kauzmann, 1959). For macromolecular interactions that combine Coulombic/van der Waals associations, both a reversal of the van der Waals interaction and a formal charge neutralization (pH increase or decrease) would be necessary to lower binding affinities. The data in Table III exhibit the effect of surface tension reduction (increasing 1-propanol addition on K_1, K_2, and $\Delta G°'$). We found it necessary to lower the ionic strength to that within the Debye–Hückel range to permit examination of this effect while maintaining the pH near neutrality. As is evident for all three mAb's, the reduction in macroscopic affinity constants

Table III: Effect of 1-Propanol on Macroscopic Binding Affinities and Free Energies. Interaction with O^6-Ethyl-2′-deoxyguanosine

antibody	γ^b	K_1	K_2	$\Delta G°'$
ER-6	71.97[c]	3.22×10^8	2.59×10^{16}	-11.21 ± 0.46
	49.30[d]	1.62×10^8	6.56×10^{15}	-10.78 ± 0.52
	24.30[e]	2.74×10^7	1.88×10^{14}	-9.73 ± 0.35
ER-3	71.97[c]	2.82×10^8	1.99×10^{16}	-11.11 ± 0.07
	49.30[d]	2.54×10^8	1.61×10^{16}	-11.05 ± 0.25
	24.30[e]	2.14×10^7	1.14×10^{14}	-9.58 ± 0.31
EM-1	71.97[c]	3.30×10^7	2.72×10^{14}	-9.84 ± 0.14
	49.30[d]	9.76×10^6	2.38×10^{13}	-9.12 ± 0.12
	24.30[e]	4.58×10^6	5.24×10^{12}	-8.67 ± 0.12

[a] Conditions for all values in the table are as follows: pH 6.8, 1×10^{-2} mM phosphate, 1×10^{-1} mM NaCl. [b] Surface tension expressed in dyn/cm. [c] Corresponds to 0% 1-propanol. [d] Corresponds to 4% 1-propanol. [e] Corresponds to 50% 1-propanol.

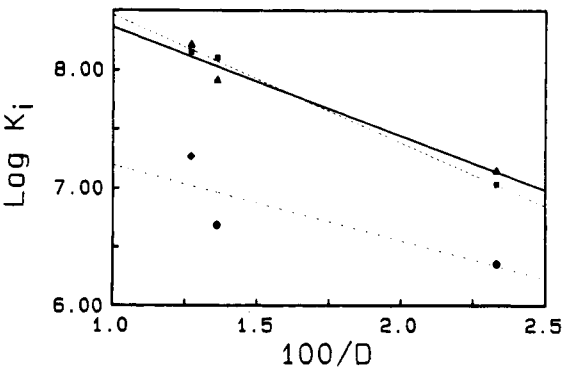

FIGURE 3: Dielectric behavior of ER-6, ER-3, and EM-1 monoclonal antibodies with O^6-EtdGuo on the log K_i as a function of 1-propanol addition, at pH 6.8, 1×10^{-2} mM phosphate, and 1×10^{-1} mM NaCl. Symbols denote same connotations as in Figure 1.

and $\Delta G°'$ is significant, indicative of the presence of the van der Waals force. Since affinity reduction was achieved by surface tension alteration alone and the apparent lack of pH dependence (Table I), we found it unnecessary to examine any other pH/surface tension permutations. It is worth noting that examination beyond 50% propanol was not possible due to irreversible mAb denaturation and nitrocellulose filter paper binding deterioration to unacceptable levels.

The 1-propanol data presented in Table III can also be examined with respect to the dielectric constant of the mixed aqueous–alcohol solvent systems. The dielectric constants for the 1-propanol–water systems were calculated from interpolation of the data by Akerlof (1932) at 20 °C. As mentioned previously, the ionic strength of the buffer system utilized in these experiments (1×10^{-2} mM phosphate, 1×10^{-1} mM NaCl) is near the Debye–Hückel limit and can be considered to approximate a pure 1-propanol–aqueous system (Laidler & Landskroener, 1954). Figure 3 is a plot of the effect of 1-propanol on the log of the intrinsic affinity constant as a function of the dielectric constant, for O^6-EtdGuo interaction with the three mAb's. Many investigators, such as Glasstone et al. (1941), have developed the theory for the treatment of reaction rates, and hence equilibria, under conditions where the bulk dielectric constant is altered. In general, the theory based on Coulomb's law for ions in solution is

$$F \equiv z_{1\epsilon} z_{2\epsilon}/Dr^2 \qquad (17)$$

where the force (F) between two ions is defined by $z_{1\epsilon}$ and $z_{2\epsilon}$, the ionic charges separated by distance r in a medium of dielectric constant D. Analysis of this equation shows that two unlike charges in the presence of a solution with a lowered dielectric constant compared with aqueous solution will experience an increase in the attractive force and hence an increase in their affinity toward one another. Conversely, for

Table IV: Temperature Dependence of Macroscopic Binding Affinities and Free Energies[a]

antigen		temp (°C) 7	14	25	37
		ER-6			
O^6-EtdGuo	$K_1 \times 10^{-8}$	17.20	7.10	3.22	0.85
	$K_2 \times 10^{-16}$	74.00	12.60	2.59	0.18
	$\Delta G^{\circ 1}$	−11.45 ± 0.13	−11.23 ± 0.27	−11.21 ± 0.46	−10.82 ± 0.17
O^6-MedGuo	$K_1 \times 10^{-7}$	7.74	3.26	1.36	0.26
	$K_2 \times 10^{-14}$	15.00	2.66	0.46	0.01
	$\Delta G^{\circ 1}$	−9.72 ± 0.10	−9.61 ± 0.13	−9.32 ± 0.12	−8.60 ± 0.31
		ER-3			
O^6-EtdGuo	$K_1 \times 10^{-8}$	13.30	6.56	2.82	0.97
	$K_2 \times 10^{-16}$	44.20	10.80	1.99	0.24
	$\Delta G^{\circ 1}$	−11.30 ± 0.17	−11.18 ± 0.19	−11.11 ± 0.07	−10.90 ± 0.14
O^6-MedGuo	$K_1 \times 10^{-8}$	1.92	1.37	0.80	ND[b]
	$K_2 \times 10^{-16}$	0.92	0.47	0.16	ND[b]
	$\Delta G^{\circ 1}$	−10.23 ± 0.14	−10.28 ± 0.13	−10.36 ± 0.08	ND[b]
		EM-1			
O^6-EtdGuo	$K_1 \times 10^{-7}$	15.00	9.74	3.30	0.64
	$K_2 \times 10^{-14}$	56.20	23.70	2.72	0.10
	$\Delta G^{\circ 1}$	−10.09 ± 0.31	−10.09 ± 0.12	−9.84 ± 0.14	−9.22 ± 0.16
O^6-MedGuo	$K_1 \times 10^{-7}$	1.37	1.31	1.03	ND[b]
	$K_2 \times 10^{-14}$	0.47	0.43	0.27	ND[b]
	$\Delta G^{\circ 1}$	−8.76 ± 0.11	−8.95 ± 0.33	−9.15 ± 0.03	ND[b]

[a] Conditions for all values in the table are as follows: pH 7.0, 10 mM phosphate, 100 mM NaCl. [b] ND = not determined; K_i values converged at less than 10^6.

Table V: Thermodynamic Parameters for Complex Formation[a]

reactants	$\Delta H^{\circ 1}$[b]	standard values $\Delta S^{\circ 1}$[c]	$\Delta G^{\circ 1}$[d]	unitary values[e] ΔS^u[f]	ΔG^u
ER-6, O^6-EtdGuo	−17.03 ± 1.57	−19.53	−11.21	−11.55	−13.59
ER-3, O^6-EtdGuo	−15.18 ± 0.39	−13.66	−11.11	−5.68	−13.49
EM-1, O^6-EtdGuo	−18.60 ± 3.10	−29.40	−9.84	−21.42	−12.22
ER-6, O^6-MedGuo	−20.66 ± 2.75	−38.05	−9.32	−30.07	−11.70
ER-3, O^6-MedGuo	−8.37 ± 0.53	6.68	−10.36	14.66	−12.74
EM-1, O^6-MedGuo	−2.72 ± 1.40	21.58	−9.15	29.56	−11.53

[a] Conditions for all values in the table are as follows: pH 7.0, 10 mM phosphate, 100 mM NaCl, 25 °C. [b] Apparent enthalpy in kcal mol^{-1}. [c] Apparent entropy in cal deg^{-1} mol^{-1}. [d] Apparent free energy in kcal mol^{-1}. [e] Corrected for effects of concentration units. [f] Unitary entropy in eu mol^{-1}.

two like charges, the same decrease in dielectric constant will result in an increase in the repulsive force and consequent decrease in affinity. The results presented in Figure 3 demonstrate the latter situation for all three mAb's with O^6-EtdGuo in the presence of increasing concentrations of 1-propanol (with decreasing D). Calculation of these slopes results in values of −0.92, −1.08, and −0.65 for ER-6, ER-3, and EM-1, respectively, while as a comparison the interaction of ammonium and cyanate ions to give urea in a water–glycol solvent system yields a positive slope of 0.77 (Amis, 1951). The positive slope for the ammonium/cyanate ion is expected for oppositely charged ions.

These dielectric results for O^6-EtdGuo interaction taken in conjunction with the sodium chloride effect demonstrate the lack of formal charge association (shallow sodium chloride slopes) but do strongly implicate dipole–dipole or ion–dipole interactions (steep dielectric slopes) as force contributors for O^6-EtdGuo interaction with the three mAb's.

Temperature Dependence. Table IV evaluates the $\Delta G^{\circ 1}$ temperature dependence for all three mAb's with both antigens, while Figure 4 exhibits the resulting van't Hoff plots (eq 12). The van't Hoff plots were analyzed by a linear least-squares routine, and the uncertainty in the enthalpy was determined by error propagation. The enthalpic values are given in Table V, in kcal mol^{-1}. For the most part, the $\Delta G^{\circ 1}$ values were evaluated at four temperatures, unless otherwise indicated, in standard buffer conditions. The apparent linearity of the plots usually indicates the lack of any heat capacity changes although Benzinger (1971) has pointed out that integration of the heat capacity with respect to temperature from absolute zero is prerequisite for an accurate evaluation. Alternatively, a very small ΔC_p may be the result of compensatory temperature effects on the enthalpies of complex formation or other ion-release processes (Hinz, 1983).

The resulting macroscopic affinities are all larger at lower temperatures, although a variation in the van't Hoff slopes is evident (Figure 4). The general trend of strongly favorable enthalpic terms for O^6-EtdGuo interaction is different from that of O^6-MedGuo interaction. Analysis of the shallow slopes results in significantly lower enthalpies (−8.37 and −2.72 kcal mol^{-1} for ER-3 and EM-1, respectively) for O^6-MedGuo interaction compared with O^6-EtdGuo interaction (−15.18 and −18.60 kcal mol^{-1} for ER-3 and EM-1, respectively). The enthalpies for ER-6 interaction with either O^6-EtdGuo or O^6-MedGuo are nearly identical (−17.03 and −20.66 kcal mol^{-1}) within the error ranges listed. The net effect of this phenomenon results in large negative entropic values for O^6-EtdGuo interaction with all three mAb's (as well as O^6-MedGuo interaction with ER-6) and an entropic reversal due to the low enthalpic values for O^6-MedGuo interaction with ER-3 and EM-1 (Table V).

Since macromolecular interactions in general are the result of the formation and rupture of many types of bonds with water and between the macromolecules themselves, it is desirable to eliminate from entropy calculations those terms that do not depend on structural modifications but are related to

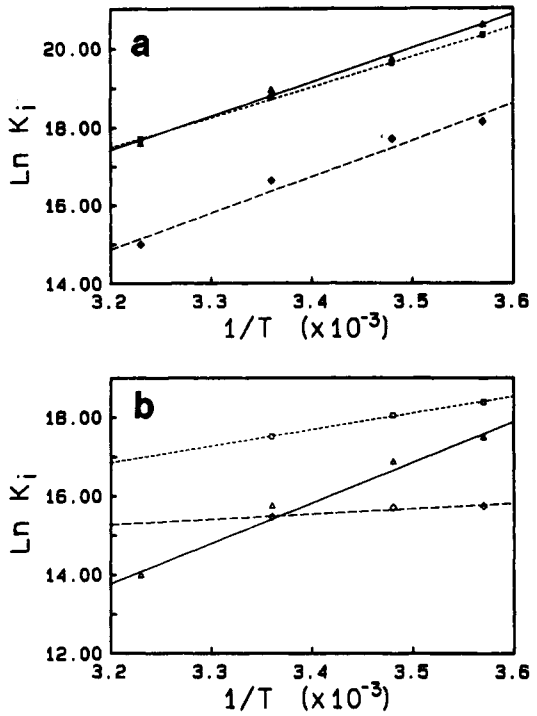

FIGURE 4: van't Hoff analysis of O^6-EtdGuo (a) and O^6-MedGuo (b) interactions with monoclonal antibodies ER-6, ER-3, and EM-1 at pH 7, 10 mM phosphate, and 100 mM NaCl. Symbols denote same connotations as in Figure 1. Slopes were curve fit by linear least-squares analysis to eq 12. Tables IV and V list the derived values.

the mixing of the macromolecules with the solvent. This mixing term has been known as the entropy of mixing and can be eliminated through the concept of unitary entropy (Mukker, 1984). The cratic contribution to the entropy of mixing for 1 gm of molecules per liter of water (55.6 mol) is R ln 55.6 = 7.89 cal deg^{-1} mol^{-1} for dilute solutions. The apparent molar entropy calculated from

$$\Delta S^{\circ 1} \equiv (\Delta H^{\circ 1} - \Delta G^{\circ 1})/T \qquad (18)$$

can be corrected by the cratic contribution to yield the unitary entropy

$$\Delta S^{u} = \Delta S^{\circ 1} + [(n-1)(7.98)] \text{ (cal deg}^{-1} \text{ mol}^{-1}) \qquad (19)$$

where n is the number of degrees of freedom for the interaction (n = 2 for mAb plus antigen) (Kauzmann, 1959; Valdes & Ackers, 1977). Values for the unitary entropy and corresponding unitary free energy are given in Table V. Comparison of the thermodynamic parameters finds that all values of $\Delta H^{\circ 1}$ and most ΔS^{u} values are negative and favorably contribute to ΔG^{u} together. From the ΔS^{u}, it is also evident that those negative $\Delta S^{\circ 1}$ values remain in negative ΔS^{u} and hence are true ordering processes and entropically disfavored. A similar argument can be applied for the two positive ΔS^{u} contributions (EM-1 and ER-3 with O^6-MedGuo), although those processes are entropically favored (large, positive ΔS^{u} values). Comparison of the two sets (enthalpic vs. entropic control) of thermodynamic parameters finds that the enthalpically controlled reactions fit well into the pattern described by the summation of terms for van der Waals interactions ($-\Delta G$, $-\Delta S$, $-\Delta H$) while the entropically controlled reactions fit into the pattern characteristic of charge association ($-\Delta G$, $+\Delta S$, $\pm\Delta H$) (Ross & Subramanian, 1981). In the case of the enthalpically controlled reactions, formal charge association processes as the dominant energetic terms were ruled out (Figure 2). These reactions were, however, found to be constant with the 1-propanol investigation and subsequent evaluation of the dominance of the van der Waals forces. The two entropically controlled reactions were found to be consistent with the sodium chloride results, in agreement with the thermodynamic parameters characteristic for ionic or formal charge association electrostatics. In neither situation were the thermodynamic parameters found to be consonant with the hydrophobic effect as the dominant force.

Discussion

These novel investigations of mAb-alkylated deoxyguanosine complexes provide thermodynamic evidence for those dominant forces involved in the epitope binding schemes, based upon the results of varying the pH, sodium chloride concentration, 1-propanol concentration, and temperature. The apparent lack of a pH dependence on the free energies of binding for all three mAb's may not provide a true reflection of the potentially ionizable groups involved in complex formation. The free energy of oligosaccharide binding to lysozyme at 25 °C has been found to vary only slightly between acidic and neutral pH, while microcalorimetric enthalpic results undergo large changes (Hinz, 1983). Since the phosphate buffering capacity is inherently larger than the macromolecule intrinsic buffering capacity, it is sometimes difficult to ascertain pH effects from the free energies. Thus it is a necessary consequence to perform microcalorimetric measurements both to determine pH effects and to validate the assumptions made previously for van't Hoff enthalpy calculation (Ross & Subramanian, 1981). Such investigations are under way and will be presented elsewhere. The sodium chloride results, in conjunction with the 1-propanol experiments, provide evidence for the dominant forces involved in complex formation, which is supplemented by the summation of thermodynamic parameters (Table V). The differential O^6-EtdGuo/O^6-MedGuo results for ER-3 and EM-1 imply alternate dominant forces at work involved in either specific or nonspecific antigen complex formation. This is in contrast to ER-6, which binds both antigens with the same dominant forces. From the data, we can state that formal charge association forces are not dominant for O^6-EtdGuo interaction with any of the three mAb's, although dipole–dipole or ion–dipole forces contribute. The dominant effect however from the surface tension analysis as well as the enthalpic and entropic results appears to be van der Waals forces. Alternatively, ER-3 and EM-1 interaction with O^6-MedGuo (compared to ER-6 with O^6-MedGuo) from the sodium chloride results and thermodynamic parameters appears to be under the control of formal charge electrostatics. Thus, while we would like to state definitively that formal charge electrostatics dominate in one instance, while van der Waals forces drive the other reactions, it must be remembered that the observed energetics of these binding reactions arise from the sum of many possible contributions, some of which undoubtedly cancel. So while we may conclude that formal charge association is not significant for O^6-EtdGuo interaction (and O^6-MedGuo interaction with ER-6), we cannot definitively ascertain the roles of van der Waals and other nonformal electrostatic contributions for these complexes. By the same accord, we cannot utilize the consistence of ER-3 and EM-1 sodium chloride and thermodynamic parameters to assert that formal charge association is dominant in these binding reactions.

This mAb-alkylated nucleoside system is particularly interesting in light of the fact that the binding ratios for ER-3 and EM-1 are small and the thermodynamic parameters for O^6-EtdGuo and O^6-MedGuo switch from enthalpic to entropic control, while the large binding ratio exhibited for ER-6 which delineates strong specificity is totally under enthalpic control

for both O^6-EtdGuo and O^6-MedGuo. Such results, indicative of compensatory forces at work, are rather unexpected since ER-3 and EM-1 are rat and mouse derived and are expected to have less primary sequence homology than the rat mAb's ER-6 and ER-3. Further structural investigation through NMR may shed more light on these findings.

ACKNOWLEDGMENTS

We thank Dr. Benjamin Turner for instruction in nonlinear least-squares analysis and Dr. D. Wayne Bolen for his many helpful discussions concerning the dielectric effect. A very special thank you is extended to Dr. Gary K. Ackers for his interest, intellectual support, and computer facilities without which the data analysis would have been impossible. Finally, our thanks are extended to Litton Bionetics for supplying our laboratory with UPC120TA myeloma antibody and syngenic BALB/cπ mice.

Registry No. O^6-EtdGuo, 50704-46-6; O^6-MedGuo, 964-21-6.

REFERENCES

Adair, G. S. (1925) *J. Biol. Chem. 63*, 529–545.

Adamkiewicz, J., Prosvziok, W., Eberhardt, W., Langenberg, V., & Rajewsky, M. F. (1982) *Banbury Report 13* (Bridges, B. A., Butterworth, B. E., & Weinstein, I. B., Eds.) pp 265–276, Cold Spring Harbor Laboratory, Cold Spring Harbor, NY.

Akerlof, G. (1932) *J. Am. Chem. Soc. 54(11)*, 4139–5125.

Amis, E. S. (1951) *J. Chem. Educ. 29*, 337–353.

Baan, R. A., Schoen, M. A., Zaalberg, O. B., & Lohman, P. H. M. (1982) *Mutagens in our Environment*, pp 111–124, Liss, New York.

Benzinger, T. H. (1971) *Nature (London) 229*, 100–102.

Brenowitz, M., Senear, D. F., Shea, M. A., & Ackers, G. K. (1986) *Methods Enzymol. 130*, 132–181.

Bruck, C., Portelle, D., Glineur, C., & Bollen, A. (1982) *J. Immunol. Methods 53*, 313–319.

Cantor, C. R., & Schimmel, P. R. (1980) in *Biophysical Chemistry, The Behaviour of Biological Macromolecules*, pp 1241–1246, W. H. Freeman, San Francisco, CA.

Casperson, G. F., & Voss, E. W. (1983) *Mol. Immunol. 20(6)*, 581–588.

Duane, M. P. (1972) *Eur. J. Biochem. 26*, 207–211.

Erlanger, B. F., & Beiser, S. M. (1964) *Proc. Natl. Acad. Sci. U.S.A. 52*, 68–74.

Ey, P. L. (1978) *Immunochemistry 15*, 429–430.

Garvey, J. S., Cremer, N. E., & Sussdorf, D. H. (1977) in *Methods in Enzymology*, 3rd ed., pp 293–297, W. A. Benjamin, New York.

Glasstone, S., Laidler, K. J., & Eyring, H. (1941) in *The Theory of Rate Processes*, pp 418–443, McGraw-Hill, New York.

Hamaker, H. C. (1937) *Physica (Amsterdam) 4(10)*, 1059–1072.

Hinz, H. J. (1983) *Annu. Rev. Biophys. Bioeng. 12*, 285–317.

Hobart, M. J., & McConnell, I. (1975) in *The Immune System*, pp 1–33, Blackwell Scientific Publications, Oxford.

Johnson, M. L., Halvorson, H. R., & Ackers, G. K. (1976) *Biochemistry 15*, 5363–5371.

Johnston, M. I., Imai, J., Lesiak, K., Jacobsen, H., Sawai, H., & Torrence, P. F. (1985) *Biochemistry 24*, 4710–4718.

Kauzmann, W. (1959) *Adv. Protein Chem. 14*, 1–63.

Kohler, G., & Milstein, C. (1976) *Nature (London) 256*, 495–497.

Laemmli, U. K. (1970) *Nature (London) 227*, 680–685.

Laidler, K. J., & Landskroener, P. A. (1954) *Trans. Faraday Soc. 52*, 200–209.

Mukker, T. K. S. (1984) *CRC Crit. Rev. Biochem. 16(2)*, 133–167.

Muller, R., & Rajewsky, M. F. (1980) *Cancer Res. 40*, 887–896.

Muller, R., & Rajewsky, M. F. (1981) *J. Cancer Res. Clin. Oncol. 102*, 99–113.

Poirier, M. C. (1981) *JNCI, J. Natl. Cancer Inst. 67*, 515–519.

Porschke, D., & Rauh, H. (1983) *Biochemistry 22*, 4737–4745.

Potter, M. (1972) *Immunol. Rev. 52(3)*, 631–719.

Rajewsky, M. F., Muller, R., Adamkiewicz, J., & Prosdziok, W. (1980) in *Carcinogenesis: Fundamental Mechanisms and Environmental Effects* (Pullman, B., Ts'o, P. O. P., & Gelboin, H., Eds.) pp 207–218, Reidel, Dordrecht, Holland.

Riggs, A. D., Bourgeois, S., & Cohn, M. (1970) *J. Mol. Biol. 53*, 401–417.

Ross, P. D., & Subramanian, S. (1981) *Biochemistry 20*, 3096–3102.

Sorenson, H. W. (1980) in *Parameter Estimation*, p 65, Marcel Dekker, New York.

Tanford, C. (1969) *J. Mol. Biol. 39*, 539–544.

Turner, B., Pettigrew, D., & Ackers, G. (1981) *Methods Enzymol. 76*, 596–628.

Valdes, R., & Ackers, G. K. (1977) *J. Biol. Chem. 252(1)*, 74–81.

Van Heyninger, V., Brock, D. J. H., & Van Heyninger, S. (1983) *J. Immunol. Methods 62*, 147–153.

van Oss, C. J., Absolom, D. R., Grossberg, A. L., & Newmann, A. W. (1979) *Immunol. Commun. 8(1)*, 11–29.

Visser, J. (1972) *Adv. Colloid Interface Sci. 3*, 331–363.

Weast, R. D. (1981) in *Handbook of Chemistry and Physics*, p D-44, CRC Chemical Rubber Co., Cleveland, OH.

Weir, D. H. (1978) in *Immunochemistry*, Vol. 1, pp 6.0–6.102, Blackwell Scientific Publications, Oxford.

Woodbury, C. P., & von Hippel, P. H. (1983) *Biochemistry 22*, 4730–4737.